Fast Multichannel Precision Thermometer

Hans-Georg Schweiger, *Member, IEEE*, Michael Multerer, and Heiner Jakob Gores

***Abstract*—This paper describes a fast multichannel precision thermometer working in a temperature range from -50 °C to $+40$ °C. Thermistors are used as temperature sensing elements. A detailed discussion of the choice of thermistor and design of the circuitry is given. It is shown that accuracy similar to that of calibrated platinum thermometers can be achieved by calibration of thermistors. During our tests, the accuracy of the thermometer was both mathematically and experimentally analyzed in detail. The stability of 30 thermistors after six months of laboratory use was analyzed. Deviations smaller than 30 mK in the range from -50 °C to $+10$ °C were observed.**

***Index Terms*—NTC, precision thermometry, resistance thermometer, temperature measurement, temperature sensor, thermistor, thermometer.**

I. Introduction

GENERALLY, platinum thermometers are used in high precision thermometry showing superior results in long-term stability and reproducibility. Therefore, they are used to interpolate between the fixed points of the ITS-90 temperature scale [1] and [2]. However, their small temperature coefficient of about 3.9×10^{-3} 1/K [3] entails a cumbersome measurement circuitry. Generally, the resistance of these devices is determined by a type of bridge circuit such as the classical Kohlrausch bridge or a transformer bridge. However, these circuits are too slow and bulky if temperature has to be measured at 30 channels for every few seconds. Even worse, high precision platinum thermometers that are traceable to national standards are wire wound types that have too large dimensions, and as a consequence, a time constant that is too large to achieve a good time resolution. Thin-film platinum resistors would overcome this problem, but they do not meet the requirements given by the Bureau International Des Poids Et Mesures, see [4] and [5]. Hence, the compatibility with standards is lost but the disadvantages of the small temperature coefficient remain. In the apparatus described in this paper, thermistors are used as temperature sensing elements due to their large temperature coefficient (typical values between -0.03 and -0.06 1/K [6]), which, in comparison to platinum thermometers, is more than ten times larger. Due to these properties, the complexity of circuit can be reduced; a simple voltage divider circuit, instead of a bridge circuit, can be used. This approach also simplifies recording because voltages can be easily digitalized and then transmitted to a computer and recorded.

However, thermistors have a bad reputation in high precision thermometry because they are assumed to have poor long-term stability, but only little evidence is given in literature [7]. In contrast to this assumption, dating presumably back to former times, they can be very stable under specific conditions, e.g., when they are applied at a constant temperature, see [8] and [7], where stabilities in the range of ± 200 μK/1000 h have been reported [7]. In [9] and [10], a thermistor-based thermometer is presented whose measurement uncertainty is claimed to be 10 mK, but no further evidence is given. Resistance fluctuations are caused by changes in the microstructure of the thermistor material [11], typically a metal oxide.

Due to improvements of this material, particularly its microstructure [11] and the development of a special cutting technique [11], the reliability and interchangeability of thermistors have been strongly improved. For example, Accu-Curve thermistors of Rhopoint Components Ltd. or the BetaCurve thermistors from BetaTHERM Corporation show an accuracy of up to 0.1 °C [12] without calibration.

The thermometer described in this paper is used in an apparatus for the determination of phase diagrams of solvent mixtures and electrolyte solutions for batteries and double-layer capacitors. With this apparatus, classical thermal analysis is performed. In this method, the substance under test is exposed to time-variant temperature (typically linear cooling or heating profiles). The bulk temperature of the substance is recorded. If a phase change in the substance occurs, energy will be consumed or released. Due to this effect, a deviation of the bulk temperature of the substance and the temperature of the surrounding is observed. Due to this effect, a horizontal section in the time temperature function of pure substances is observed at the melting point. For liquid electrolytes, a change in the slope will result if the composition of the liquid phase changes, when crystals are formed. A detailed description of this method is given by Skau and Arthur [13].

For the investigation of electrolyte solutions, a temperature range from -50 °C to $+40$ °C is desirable. High resolution of 1 mK is necessary for studying supercooling phenomena. The accuracy of the system was attempted to reach the range of standard platinum resistance thermometers, typically 25 mK, particularly at lower temperatures. A fast measurement rate of one sample per second is essential for a useful time resolution.

II. Theory of Operation

The thermometer described in this paper is based on a voltage divider consisting of a thermistor and a precision resistor.

Manuscript received February 28, 2006; revised April 15, 2007. This work was supported in part by GAIA Akkumulatorenwerke GmbH, D-99734 Nordhausen, Germany.

H.-G. Schweiger was with the Institut für Physikalische und Theoretische Chemie, Universität Regensburg, 93040 Regensburg, Germany. He is now with Temic Automotive Electric Motors GmbH, 10553 Berlin, Germany (e-mail: Hans-Georg@Schweiger.name).

M. Multerer and H. J. Gores are with the Institut für Physikalische und Theoretische Chemie, Universität Regensburg, 93040 Regensburg, Germany (e-mail: Michael.Multerer@chemie.uni-regensburg.de; Heiner.Gores@chemie.uni-regensburg.de).

Digital Object Identifier 10.1109/TIM.2007.904480

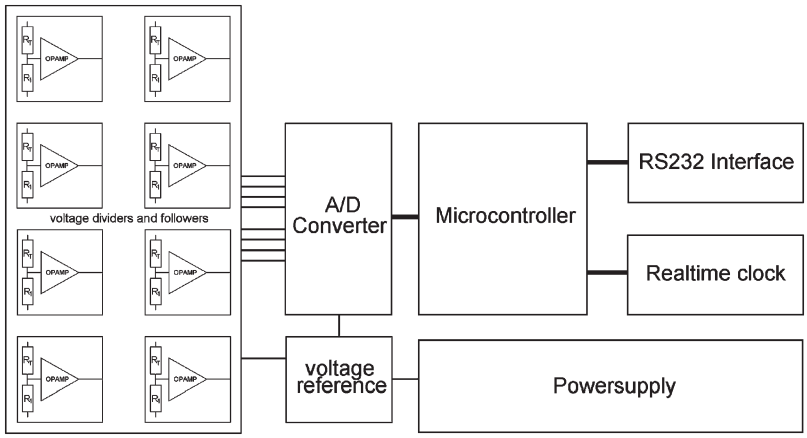

Fig. 1. Overview of the thermometer.

This voltage divider is used for converting the temperature-dependent resistance of the thermistor in a temperature-dependent voltage. The voltage is measured with an analog-to-digital converter (ADC) that is controlled by a microcontroller. Temperature is calculated with the help of the Steinhart–Hart equation (1). For obtaining accuracy better than 0.1 °C, the parameters of this equation, which were supplied by the manufacturer, were improved by calibration. The thermometer contains four ADCs with eight channels. Each channel is connected to a voltage divider, so a 32-channel thermometer results. Because two channels were used for internal temperature measurement, 30 external thermistors can be connected. In Fig. 1, an overview of the thermometer is given.

To save space, only one ADC and eight dividers with followers are shown.

III. Description of the System

A. Sensor

BetaTHERM BetaCurve thermistors are used as temperature sensing elements. These sensors are interchangeable in the range of 0 °C to 70 °C if the calibration function of the manufacturer is used [12]. The deviations are less than 0.1 K. Their exceptional long-term stability of −0.097 K (within nine years if the thermistor is kept at 75 °C [14]), which is claimed by the manufacturer, recommends them for replacing platinum sensors. Their accuracy can be improved by individually calibrating the sensors. The stability of these sensors is demonstrated in the experimental section of this paper, where a maximum deviation of 30 mK after usage of the thermometer (several rapid cycles between +40 °C and −50 °C) for six month was obtained.

The temperature dependence of thermistors, which is given by Steinhart and Hart, is typically described by

$$\frac{1}{T} = A + B \cdot \ln \frac{R_T}{R_0} + C \cdot \left(\ln \frac{R_T}{R_0} \right)^3 \text{ [15]} \qquad (1)$$

where $R_0 = 1\Omega$, R_T is the resistance at temperature T, and A, B, and C are fitting parameters.

To avoid erroneous results caused by self-heating of the thermistor, as shown in Section III-B, the current through the thermistor must be reduced.

BetaTHERM offers BetaCurve thermistors with a resistance range from 2.2 kΩ to 1 MΩ at 25 °C. Due to the exponential increase of the thermistor's resistance at lower temperatures, particularly for types with extremely high resistance, it is a cumbersome task to avoid parasitic resistances, e.g., a 1-MΩ (25 °C)-type thermistor shows 0.3 GΩ at −60 °C. Therefore, the 30K6A1 thermistor was chosen, showing a resistance of 30 kΩ at 25 °C and about 5.4 MΩ at −60 °C; hence, sufficient low power dissipation is combined with manageable resistances.

For this thermistor, the manufacturer states the standard values of Steinhart and Hart coefficients to be $A = 1.068981 \times 10^{-3}$ 1/K, $B = 2.120700 \times 10^{-4}$ 1/K, and $C = 9.019537 \times 10^{-8}$ 1/K.

Due to its fast response of 1 s in stirred liquids [12], high-speed thermometry is made possible.

B. Voltage Divider

Temperature is transformed by the thermistor to a resistance. Classically, a resistance is measured by balancing bridges of Wheatstone or Kohlrausch type or with transformer bridges with alternating current, e.g., [16]. If data are collected by computer, the decades of the bridge must be motorized, or self-calibrated. However, these bridges are too slow; they typically provide a data rate of one measurement per 2 s or slower. As an alternative, a self-balancing bridge could be applied, as described in [16] and [17]. Because of the large temperature coefficient of thermistors, a much simpler approach can be used to determine the resistance. A simple voltage divider, as shown in the left part of Fig. 2, transforms the resistance of the thermistor into a voltage that can be easily measured with an ADC. This divider consists of the thermistor R_T and a reference resistor R_1.

The series resistor R_1 generates the voltage drop, which is measured by the ADC.

The voltage drop V_{R1} is calculated by

$$U = \frac{R_1}{R_1 + R_T} U_{\text{REF}}. \qquad (2)$$

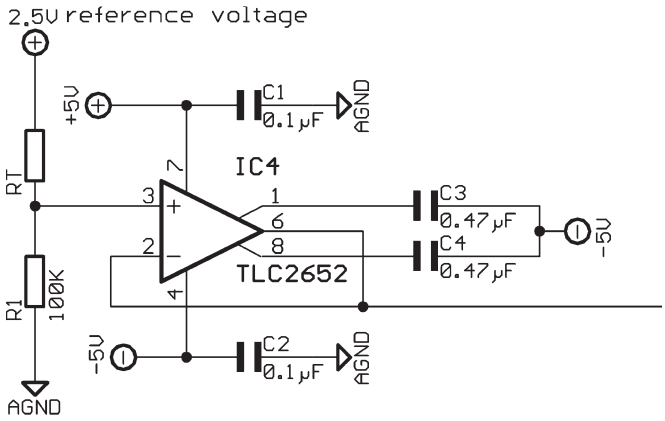

Fig. 2. Voltage divider circuit with follower.

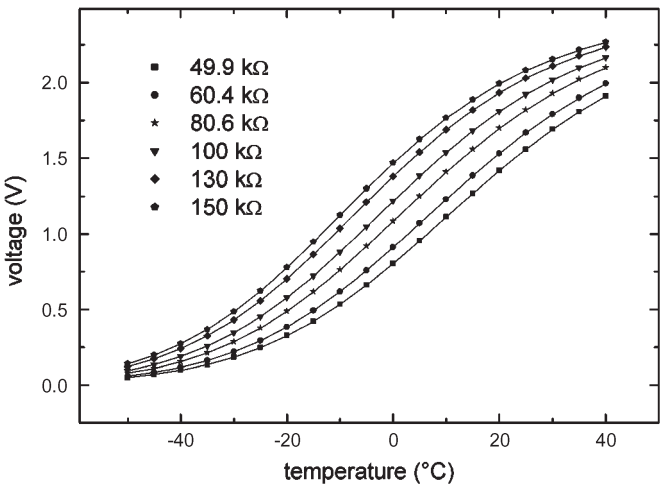

Fig. 3. Temperature dependence of the voltage divider with different reference resistors.

The temperature dependence of the voltage of the divider is obtained by solving (1) for R_T, with the aid of the method of Cardano, and then transferring the result into (2), yielding (3), as shown at the bottom of the page. This transformation also gives a coarse linearization of the temperature dependence of the response of the thermistor [18]–[20]. As the correlation between temperature and measured voltage is numerically done with the aid of a computer, there is no need for this feature at the first sight, but the requirements of the dynamic range of the ADC are strongly reduced.

Combination of (1) with (2) yields to

$$T = \frac{1}{A + B \cdot \ln \frac{\frac{R_1 \cdot U_{\mathrm{REF}}}{U} - R_1}{R_0} + C \cdot \left(\ln \frac{\frac{R_1 \cdot U_{\mathrm{REF}}}{U} - R_1}{R_0} \right)^3}. \quad (4)$$

With this equation, the appertaining temperature can be calculated from the measured voltage U.

As it is obvious from Fig. 3, the slope of the function $U(\theta)$ decreases at higher temperatures, and therefore, a resolution decrease results at elevated temperatures. If this thermometer circuitry is applied for measurement of high temperatures instead of low temperatures, R_1 and the thermistor should change places in the potentiometer circuit.

To determine an appropriate value for resistor R_1, the output voltage of the voltage divider in the range of -50 °C to $+40$ °C, with different values for R_1, was calculated, see Fig. 3.

The temperature-dependent voltage should cover the dynamic range of the ADC, which is limited by its reference voltage. Because of the reasons shown in Section III-D, the ADC is fed by the same reference voltage; therefore, in the best case, the converter circuit does not limit this range. The highest resolution of temperature measurement will be achieved if the slope of the function $U(\theta)$ shown in Fig. 3 is maximal. If the slope decreases, the temperature resolution will decrease, too. As one can see in Fig. 3, the best resolution over the whole temperature range is achieved with intermediate values for R_1 without a strong decrease of the dynamic range.

The reference resistor R_1 not only generates a suitable voltage drop for the ADC but also limits the current through the thermistor. In the circuit described by O'Grady [21], a third resistor is applied for this purpose. This resistor decreases the voltage drop at the measuring resistor. Furthermore, this resistor introduces additive errors.

To avoid erroneous results caused by self-heating of the thermistor, the resistances of thermistor R_T and reference resistor R_1 must be as high as possible so that, at the thermistor, the resulting power P in the following equation will be as low as possible:

$$P = R_T \cdot \left(\frac{U_{\mathrm{REF}}}{R_T + R_1} \right)^2. \quad (5)$$

Fig. 4 shows the power dissipation at the thermistor over the temperature range from -50 °C to $+40$ °C, with various values for R_1. As expected, low power dissipation is achieved with large reference resistors, which is still small enough at intermediate resistance levels. Although all values for R_1 shown in Fig. 4 meet the zero power requirement of 100 μW given by BetaTHERM [22], we have chosen a value of 100 kΩ

$$U = \frac{R_1}{\exp\left[\sqrt[3]{-\left[\frac{\frac{(A-T^{-1})}{C}}{2} + \sqrt{\left[\frac{\frac{(A-T^{-1})}{C}}{4} \right]^2 + \left[\frac{\left(\frac{B}{C}\right)^3}{27} \right]} \right]} + \sqrt[3]{-\left[\frac{\frac{(A-T^{-1})}{C}}{2} - \sqrt{\left[\frac{\frac{(A-T^{-1})}{C}}{4} \right]^2 + \left[\frac{\left(\frac{B}{C}\right)^3}{27} \right]} \right]} + R_1} \cdot U_{\mathrm{REF}} \quad (3)$$

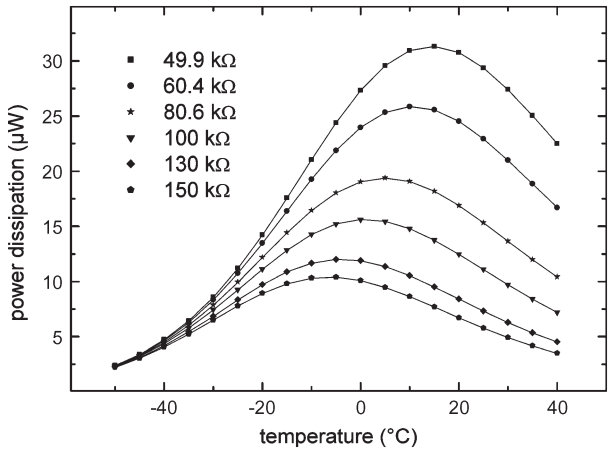

Fig. 4. Power dissipation of the thermistor at various temperatures and with different values of R_1.

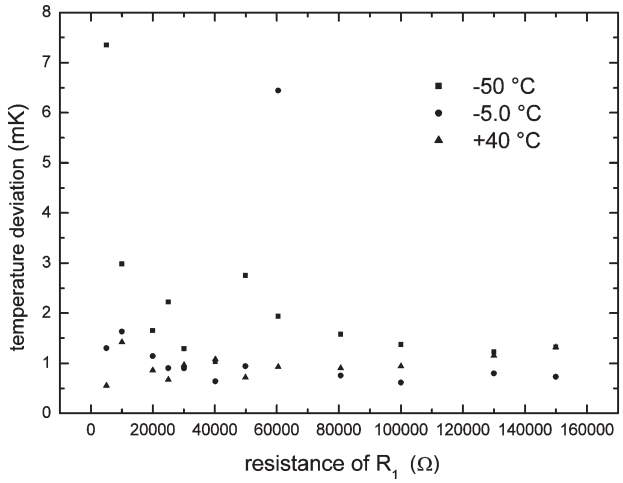

Fig. 5. Influence of R_1 to the system's noise.

for the reference resistor because this resistor gives not only a good slope over the temperature range but also a very low heat dissipation (max. 15 μW) at the thermistor.

The system noise is also influenced by the choice of the resistor. To test this effect, 12 precision resistors from Rhopoint, in the range of 50–150 kΩ, were used for R_1, whereas temperature was measured in a stirred oil bath for 2000 s. The bath temperature of our thermostat was set to -50.00 °C, -5.00 °C, and $+40.00$ °C with a fluctuation of about 1 mK. The results of these measurements are shown in Fig. 5, where the statistical spread of the measured temperature is plotted against the resistance of the reference resistor.

No real significant dependence of noise from the value of R_1 is found. Perhaps, the noise may decrease a bit with the increase of R_1. If the three points discussed above are all taken into account, an intermediate value of 100 kΩ seems suitable for the reference resistor R_1 because this provides a high resolution in combination with low noise, sufficiently low power dissipation, and availability.

In our device, a Rhopoint Econistor-type resistor of 100 kΩ with a small temperature coefficient of 3 ppm/K [23] has been chosen to reduce the errors due to changes of ambient temperature.

C. Follower

If the voltage divider is directly connected to the ADC, its output voltage will be adulterated by the low-input impedance of 39 kΩ [24] of the ADC. To overcome this problem, a follower circuit is placed between the voltage divider circuit and the ADC. This follower, as shown in the right part of Fig. 2, was realized with the chopper-stabilized operational amplifier TLC2652A from Texas Instruments Incorporated. It provides high-input impedance and low-output impedance. A chopper-stabilized operational amplifier has been chosen because of its very low offset voltage. The chopper frequency of this device is 450 Hz [25], which is rejected by the ADC as whole number multiplier of its filter frequency.

D. Voltage Reference

The voltage dividers are fed with 2.5 V generated by a Maxim MAX6325CPA precision voltage reference. This reference gives an output voltage of (2.500 ± 0.001) V with a temperature coefficient of 1 ppm and very low noise of 1.5 μVp-p (0.1–10 Hz) [26].

Errors generated by drifts of the voltage, which feed the potentiometers, formed by the thermistors and their associated R_1's, are canceled out because the same voltage reference is also used as a reference voltage for the ADC (Fig. 1). Thus, the ADC actually measures the ratio between the thermistor and R_1, which is not affected by the drift of the sensor supply voltage [27].

E. ADC

The heart of the thermometer is the ADC. The characteristic feature of this device is its resolution. As shown in Section I, a temperature resolution of 1 mK should be achieved.

The corresponding voltage resolution can be calculated by (6), as shown at the bottom of the next page.

The required resolution of the ADC, i.e., BITMAX, can be determined if (6) is set into

$$\text{BITMAX} = \log_2 \left(\frac{U_{\text{REF}}}{\Delta U} \right). \tag{7}$$

In Fig. 6, the desired resolution for the ADC is plotted for the temperature range from -50 °C to $+40$ °C.

As one can see, the ADC needs a resolution of 19 bits at least to achieve a temperature resolution of 1 mK if the divider circuit described in Section III-B is used.

Typically, sigma-delta converters are used in high-resolution applications. Due to their integrating property, they provide excellent high-frequency noise rejection. Their slower conversion speed is not critical for this application because only one measurement per second is attempted. To reduce the number of components, a multichannel ADC with an internal multiplexer is desirable.

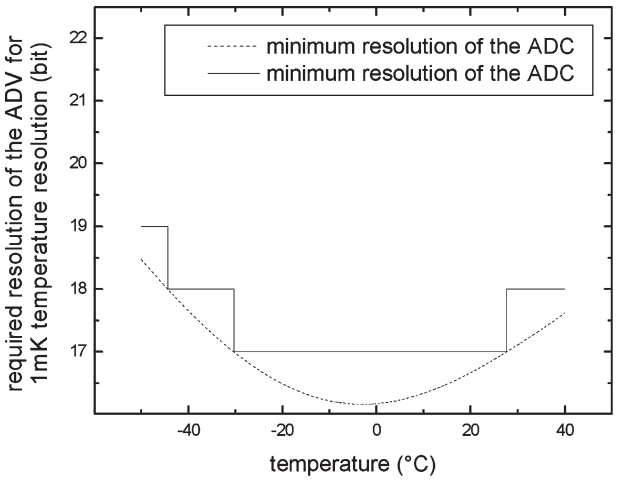

Fig. 6. Minimum resolution of the ADC to achieve 1-mK temperature resolution.

For this application, ADS1241E ADCs from Texas Instruments Incorporated were chosen. These eight-channel 24-bit sigma-delta ADCs have an internal programmable gain amplifier (PGA). With this 1-to-128 amplifier, the small output voltage of the divider circuit can be amplified, and therefore, the signal-to-noise ratio can be reduced further. In contrast to the AD7711 described in [21], the ADS1241E has much smaller offset voltage and offset drift and entails the highest contribution of the ADC to total system error. Its fastest data rate of 15 conversions/s [24] fulfills the requirements given above. Slower conversion rates would increase the accuracy of this component, but changing the channels of the ADC is time consuming so the high-speed mode is required. The four ADCs are connected via a serial peripheral interface (SPI) to the microcontroller. To ensure a synchronous operation of the four ADCs, the SPI was modified. Signals coming from microcontroller going to the ADC, like SCLK, CS, DIN, and DSYNC come from the same ports of the microcontroller and are split to each ADC: in contrast to this, each ADC has its own data signal DOUT connected to the microcontroller, which transports the results of the conversion. With this modification, the four ADCs can be simultaneously read out.

F. Microcontroller, Interface, and Additional Circuitry

An Atmel Mega16 Microcontroller is applied for controlling the four ADCs and provides the UART for the RS-232 interface. This interface is realized with Maxim MAX220 line drivers/receivers. A Dallas DS1305 real-time clock, which is also connected to the Microcontroller, is used for generating the time base for the cooling curves. The power supply of the device is realized by a conventional transformer supply. Because the thermometer is affected by noise of the supply voltages, care has to be taken in voltage regulation and filtering.

IV. Calibration

Calibration was performed by comparison with a standard thermometer. Thermistors were put into a thermostat, as described by Barthel and Wachter [28], which provides a long-term stability of about 3 mK. Temperature of the thermostat was checked with an F-250 MkII thermometer from Automatic Systems Laboratories (Milton Keynes). The appertaining platinum thermometer was calibrated by WYCO (Romsay) according to The United Kingdom Accreditation Service; a temperature accuracy of 25 mK [29] was achieved. Calibration points from $-60.00\,^{\circ}\mathrm{C}$ to $+40.00\,^{\circ}\mathrm{C}$ were taken in steps of 10 K. Equation (4) was fitted by nonlinear regression using A, B, C, and U_{REF} as parameters. Attempts to also fit the resistance R_1 by this method failed because no stable condition was found.

V. Estimation of Accuracy

The accuracy of our equipment was analyzed by several methods. First, the error induced by the components of the

$$\Delta U = \frac{R_1 \cdot U_{\mathrm{REF}}}{\exp\left[\sqrt[3]{-\left[\frac{\left(A-T^{-1}\right)}{C}+S_1\right]}+\sqrt[3]{-\left[\frac{\left(A-T^{-1}\right)}{C}-S_1\right]}\right]+R_1} - \frac{R_1 \cdot U_{\mathrm{REF}}}{\exp\left[\sqrt[3]{-\left[\frac{\left(A-(A-\Delta T)^{-1}\right)}{C}+S_2\right]}+\sqrt[3]{-\left[\frac{\left(A-(AT)^{-1}\right)}{C}-S_2\right]}\right]+R_1}$$

$$\text{with} \quad S_1 = \sqrt{\frac{\left[\frac{\left(A-T^{-1}\right)}{C}\right]}{4}+\frac{\left[\left(\frac{B}{C}\right)^3\right]}{27}}$$

$$S_2 = \sqrt{\frac{\left[\frac{\left(A-(T-\Delta T)^{-1}\right)}{C}\right]}{4}+\frac{\left[\left(\frac{B}{C}\right)^3\right]}{27}} \tag{6}$$

circuitry was analyzed by the error propagation law. In these calculations, the errors of thermistors were ignored at first; only the performance of the circuitry was analyzed. The noise of the system was experimentally determined. Finally, the total accuracy was determined by comparison with a standard thermometer.

A. Error Calculation

Our goal was to design a thermometer showing a total accuracy of 25 mK; therefore, the error of the measuring system has to be lower than 1 mK, leaving enough space for errors of the thermistor and for errors of calibration.

The error of temperature of our measuring system was estimated by the error propagation law. All errors given in the data sheets [23]–[25] of the devices applied in the system were considered. In this context, noise of the system was not taken into account, but it was experimentally determined, as shown in Section V-B. There is no need to consider manufacturing tolerances of the devices because thermistors and measurement channels were calibrated together and, therefore, do not influence the accuracy of the system. Only changes in the parameters were taken into account. Fluctuations of the ambient temperature affect the accuracy due to the temperature coefficients of the devices. These changes were taken into account in their typical range of ± 5 °C around 25 °C. Long-term drifts were considered in a timeframe of 10 000 h, which is longer than typical calibration intervals.

The error introduced by the resistor of the voltage divider can be determined by derivation of (4) to R_1, yielding

$$\Delta T_{R_1} = \left| \frac{B + 3 \cdot C \cdot \ln\left(\frac{S}{U \cdot R_0}\right)^2}{\left(A + B \cdot \ln\left(\frac{S}{U \cdot R_0}\right) + C \cdot \ln\left(\frac{S}{U \cdot R_0}\right)^3\right)^2 \cdot R_1} \right| \cdot |\Delta R_1| \tag{8}$$

where $S = R_1(U_{\mathrm{REF}} - U)$.

For obtaining the dependence of this error with measurement temperature, U has to be replaced by the right-hand side of (3).

The error of the resistor ΔR_1 consists of its temperature coefficient of 3 ppm/K [23] and its long-term stability of 35 ppm/10 000 h [23]. The dashed line in Fig. 7 shows the influence of this error on the system's performance over the whole measuring range.

The error introduced by the follower is determined in an analogous way by deriving (4) to U, yielding

$$\Delta T_{U_{\mathrm{OPAMP}}} = \left| \frac{U_{\mathrm{REF}} \cdot R_1 \cdot \left(B + 3 \cdot C \cdot \ln\left(\frac{S}{U \cdot R_0}\right)^2\right)}{\left(A + B \cdot \ln\left(\frac{S}{U \cdot R_0}\right) + C \cdot \ln\left(\frac{S}{U \cdot R_0}\right)^3\right)^2 \cdot U \cdot S} \right| \cdot |\Delta U_{\mathrm{OPAMP}}| \tag{9}$$

where $S = R_1(U_{\mathrm{REF}} - U)$.

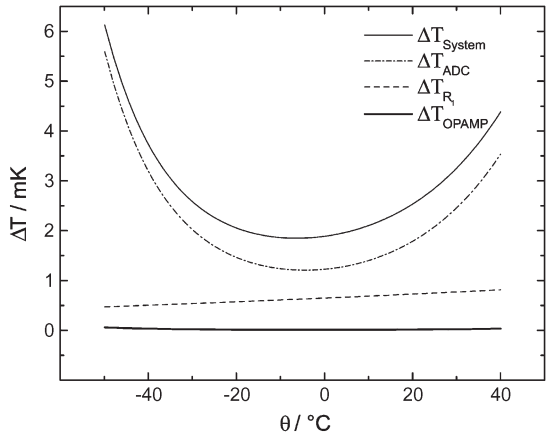

Fig. 7. Calculated errors of the measured temperature.

TABLE I
ERRORS OF THE ADC

Error	Value
Missing Codes/Bits	0
INL/%FSR	0.0015/PGA
effective resolution Bit	19
Offset drift/ppm/°C	0.02/PGA
Gaindrift ppm/°C	0.5

The error $\Delta U_{\mathrm{OPAMP}}$ is made up of the long-term drift of 0.02 μV/month [25] and its temperature coefficient of 0.03 μV/K [25]. The influence of this error on system performance is shown by the dotted line in Fig. 7, and can be calculated if U in (9) is replaced by the right-hand side of (3).

With (10), the errors generated by the ADC can be determined by

$$\Delta T_{\mathrm{ADC}} = \left| \frac{U_{\mathrm{REF}} \cdot R_1 \cdot \left(B + 3 \cdot C \cdot \ln\left(\frac{S}{U \cdot R_0}\right)^2\right)}{\left(A + B \cdot \ln\left(\frac{S}{U \cdot R_0}\right) + C \cdot \ln\left(\frac{S}{U \cdot R_0}\right)^3\right)^2 \cdot U \cdot S} \right| \cdot |\Delta U| \tag{10}$$

with $S = (U_{\mathrm{REF}} - U) \cdot R_1$.

The voltage error ΔU is caused by the error of the PGA of the ADC ΔPGA, the integral nonlinearity INL, the drift of the offset U_{offset}, and the effective resolution ΔBIT. Values are given in Table I.

The dependence of this error with the measured temperature will be obtained if the voltage U in (10) is replaced by the right-hand side of (3).

The error caused by the ADC is shown as the dashed and dotted line in Fig. 7 as a function of the measured temperature.

The errors caused by the voltage reference can be neglected because the ADC as well as the voltage dividers are fed with the same voltage reference, and therefore, changes of the reference

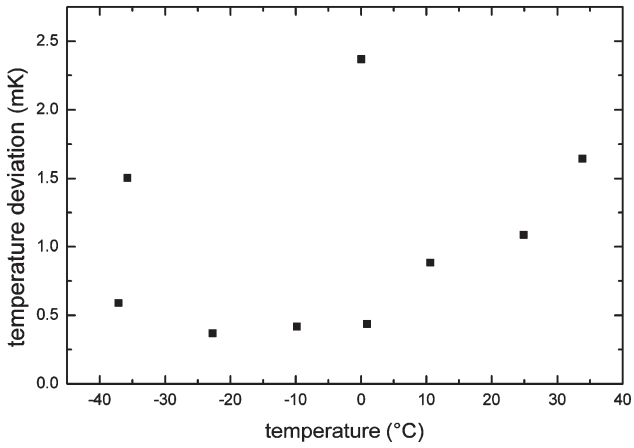

Fig. 8. Noise of the system.

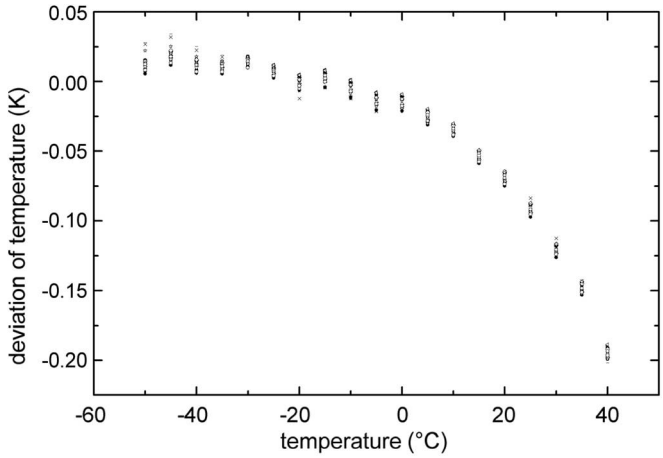

Fig. 9. Deviation of the thermistors after six months.

voltage are cancelled out and do not affect the performance of the system.

In Fig. 7, the total error $\Delta T_{\mathrm{System}}$ is shown. In this figure, the error is shown in dependence of the measured temperature. The thermometer itself is at (25 ± 5) °C. This error was calculated by summing the errors ΔT_{R1}, $\Delta T_{\mathrm{OPAMP}}$, and ΔT_{ADC}, which are also shown. The total error shows a maximum of 6 mK at -50 °C, which is far below the required limit of 25 mK. The largest contribution to the systems error is from the ADC. Therefore, choosing a better ADC would be the most successful step to optimize the circuitry. In contrast, a better Opamp or Resistor would only give slight improvements.

All error calculations were performed with the help of MAPLE. Data sheets and Maple Worksheets can be supplied on request.

B. Determination of Noise

In principle, placing the thermistors in a thermostat at a fixed temperature and measuring the temperature over a period of time could determine the noise of the whole measurement system. Because our thermostat shows fluctuations in the range of 3 mK, which is measured by a platinum resistance thermometer in an ac bridge, it is impossible to differentiate the noise of the thermometer from the noise of the thermostat.

Therefore, the noise of the measurement system was determined by simulating the temperature probes with resistors. For this purpose, 20 kΩ to 1 MΩ resistors were used, simulating temperatures in the range from -37 °C to $+35$ °C. The simulated temperatures were measured for 200 000 s, and the standard deviations of the measured temperatures were calculated. In Fig. 8, the results of these measurements are shown.

Over the whole temperature range, the noise of the thermometer is below 2.5 mK. By simulating the thermistors by regular resistors, one must take into account that the noise characteristics of these devices may differ, so the simulation shown here may only be an approximation.

C. Accuracy of the System and Stability of Thermistors

The long-term stability of the whole measurement system was checked six months after calibration. During this time, the thermistors were used in phase diagram studies where they were exposed to about 100 temperature cycles in the range -50 °C to $+40$ °C. The test of the calibration was performed the same way as the calibration described in Section IV, by placing the thermistors in the oil bath of the thermostat and determining the difference between the temperatures measured by the thermistor thermometer and the ASL reference thermometer. To prove that the calibration was working well between the calibrated temperatures, each 5 °C was checked. The results of these measurements can be seen in Fig. 9, where the deviations the temperatures measured with 30 thermistors and the reference thermometer are shown.

In the range from -50 °C to $+10$ °C, only a deviation smaller than 30 mK is observed. In this range, the multichannel thermistor thermometer is nearly as good as our platinum resistance thermometer with its accuracy of 25 mK [29]. At higher temperatures, larger deviations up to 200 mK are observed. The error distribution is ideal for our application because most of the systems we analyzed have phase transitions in the range from -50 °C to -10 °C.

The observed high long-term stability of thermistors shows that they are a good replacement for platinum resistors for our application.

VI. Conclusion

If thermistors are carefully chosen and are calibrated to a standard thermometer, stability and accuracy similar to platinum thermometers can be achieved. The stability of the thermistors is better than 30 mK in the temperature range from -50 °C to $+10$ °C.

Therefore, thermistors are suitable to replace platinum resistance thermometers in certain applications, as thermistors have smaller dimensions and faster response. Due to the higher temperature coefficient of thermistors, the complexity of circuitry is strongly reduced in contrast to platinum thermometers.

ACKNOWLEDGMENT

The authors would like to thank H. Becker for the discussion and A. Schweiger, M. Spannbauer, and F. Wudy for the editing.

REFERENCES

[1] M. L. McGlashan, "The international temperature scale of 1990 (ITS-90)," *J. Chem. Thermodyn.*, vol. 22, no. 7, pp. 653–663, 1990.
[2] *The International Temperature Scale of 1990*, 1990, Sevres, France: Bureau International Des Poids Et Mesures.
[3] G. C. M. Meijer and A. W. Herwaarden, "Thermal sensors," *Sensor Series*, 1994.
[4] *Supplementary Information of the International Temperature Scale of 1990*, 1990, Sevres, France: Bureau International Des Poids Et Mesures.
[5] *Techniques for Approximating the International Temperature Scale of 1990*, 1990, Sevres, France: Bureau International Des Poids Et Mesures.
[6] J. V. Nicholas and D. R. White, *Traceable Temperatures*. Chichester, U.K.: Wiley, 2001.
[7] P. Sydenham and G. Collins, "Thermistor controller with microkelvin stability (for strainmeter testbase temperature control)," *J. Phys. E, Sci. Instrum.*, vol. 8, no. 4, pp. 311–315, Apr. 1975.
[8] A. Sloman, P. Buggs, J. Molloy, and D. Stewart, "A microcontroller-based driver to stabilize the temperature of an optical stage to within 1 mK in the range 4–38 degrees C, using a Peltier heat pump and a thermistor sensor," *Meas. Sci. Technol.*, vol. 7, no. 11, pp. 1653–1664, Nov. 1996.
[9] V. Hans and H. Kollmeier, "Highly accurate temperature measurements, using a multi-slope analog-to-digital converter," *Elektronik*, vol. 41, no. 14, p. 43, 1992.
[10] V. Hans, "High accuracy measuring method of absolute temperatures using thermistors," in *Proc. IEEE Int. Symp. Ind. Electron.*, 1992, vol. 1, pp. 29–30.
[11] H. Schaumburg, *Sensoren*. Stuttgart, Germany: B.G. Teubner, 1992.
[12] *BetaCurve Interchangeable Thermistor Series I*, 2002, Shrewsbury, MA: BetaTHERM Corporation. [Online]. Available: http://www.betatherm.com/betacurbetachip.htm
[13] E. L. Skau and J. C. Arthur, "Determination of melting and freezing temperatures," *Phys. Methods Chem.*, vol. 5, pp. 105–198, 1971.
[14] *Stability and Reliability of Thermistors*, 2002, Shrewsbury, MA: BetaTHERM Corporation. [Online]. Available: http://www.betatherm.com/stability
[15] S. R. Hart and J. S. Steinhart, "Calibration curves for thermistors," *Deep-Sea Res.*, vol. 15, p. 497, 1968.
[16] P. Caleb and F. Wolfendale, "Impedance apparatus having lead wire resistance compensation means," U.S. Patent 3 584 296, Jun. 8, 1971.
[17] D. R. White, "A high resolution transformerless bridge," *J. Phys. E, Sci. Instrum.*, vol. 15, no. 7, pp. 753–754, Jul. 1982.
[18] A. Khan, "Linearization of thermistor thermometer," *Int. J. Electron.*, vol. 59, no. 2, pp. 129–139, 1985.
[19] C. Molee and P. Vitale, "Thermistors make good thermometers," *Electron. Des.*, vol. 26, no. 8, p. 90, 1978.
[20] W. R. Beakley, "The design of thermistor thermometer with linear calibration," *J. Sci. Instrum.*, vol. 28, no. 6, pp. 176–179, Jun. 1951.
[21] A. O'Grady, Analog Devices Technical Note, *Temperature Measurement Using a Thermistor and the AD7711 Sigma Delta ADC*, Norwood, MA: Analog Devices.
[22] *Zero-Power Resistance*, 2002, Shrewsbury, MA: BetaTHERM Corporation. [Online]. Available: http://www.betatherm.com/zero_ower.htm
[23] *Econistor 8E16&8E24*, 2002, Oxted, U.K.: Rhopoint Components Ltd.
[24] *ADS1240/ADS1241 24-Bit Analog-to-Digital Converter*, 2000, Dallas, TX: Texas Instruments Inc.
[25] *TLC2652, TLC2652A, TLC2652Y, Advanced LinCMOS Precision Chopper-Stabilized Operational Amplifiers*, 2001, Dallas, TX: Texas Instruments Inc.
[26] *MAX6325/MAX6341/MAX6350 1 ppm/°C, Low-Noise, +2,5 V/+4,096 V/+5 V Voltage References*, 2001, Sunnyvale, CA: Maxim Integrated Products Inc.
[27] H. Trietley, "All about thermistors—III," *Radio-Electron.*, vol. 56, no. 3, p. 67, 1985.
[28] J. Barthel and R. Wachter, "The temperature dependence of the properties of electrolyte solutions—I: A semiphenomenological approach to an electrolyte theory including short range forces," *Berichte der Bunsengesellschaft für Physikalische Chemie*, vol. 83, pp. 252–257, 1979.
[29] *F250 Mk II Manual*, Automatic Systems Laboratories Ltd., Milton Keynes, U.K.

Hans-Georg Schweiger (M'06) was born in Ingolstadt, Germany, in 1977. He received the Dipl. Chem. degree and the Ph.D. degree in chemistry from the University of Regensburg, Regensburg, Germany, in 2002 and 2004, respectively.

After receiving the Ph.D. degree, he was a Development Engineer for energy storage systems with EVA Fahrzeugtechnik GmbH, Munich, Germany, for nearly two years. Since the beginning of 2007, he has been with Temic Automotive Electric Motors GmbH (part of Continental Automotive Systems), Berlin, Germany, where he is responsible for the simulation of energy storage systems and for the development of algorithms for the online determination of the SOC and SOH of energy storage systems. He had several summer jobs at Audi AG, Ingolstadt, Bayer AG, Leverkusen, Germany, G+H Montage GmbH, Ingolstadt, and Zimmer Elektroanlagen GmbH, Ingolstadt. In 1994, he received a summer fellowship at the GSF-National Research Center for Environment and Health, Munich. His research interests include optimization of electrolytes for lithium ion batteries, determination of phase diagrams of electrolyte solutions, development of instrumentation for temperature and conductivity measurement, and general electrochemical instrumentation.

Dr. Schweiger is a member of the Electrochemical Society and the Gesellschaft Deutscher Chemiker.

Michael Multerer was born in Burghausen, Germany, in 1977. He received the Dipl. Chem. degree from the Universität Regensburg, Regensburg, Germany, in 2002, where he is currently working toward the Ph.D. degree at the Institut für Physikalische und Theoretische Chemie.

His current research interests include the investigation of electrolytes for lithium ion batteries concerning their electrochemical stability. The main aspects of his work are the influence of impurities such as moisture and the mechanism of degradation of the electrolytes. To elucidate electrode reactions, he is building up an electrochemical quartz microbalance suited to the special requirements of his work.

Mr. Multerer is a Student Member of the Electrochemical Society.

Heiner Jakob Gores was born in Dudweiler, Germany, in 1946. He received the Dipl. Chem. and Ph.D. degrees from the University of Saarbrücken, Saarbrücken, Germany, in 1970 and 1974, respectively.

In 1996, he was assigned as Privatdozent at the University of Regensburg, Regensburg, Germany. He has been with the Institut für Physikalische und Theoretische Chemie, Universität Regensburg, as an Assistant Professor since 1971, an Academic Director, teaching physical chemistry in laboratory courses and lectures, since 1980, and was appointed as an Adjunct Professor (apl. Prof.) in 2006. He initiated a research group that is mainly sponsored by industrial German companies such as EPCOS AG, Merck KgaA, Infineon AG, Chemetall GmbH, and Gaia Akkumulatorenwerke GmbH. He is the coauthor of several papers and reviews in his fields of interest. His current research interests include synthesis and characterization of new electrolytes for lithium ion batteries, double-layer capacitors, solar cells, and electroplating as well as electrochemical, thermodynamic, and kinetic studies of nonaqueous electrolytes, polymers, gels, and ionic liquids. Measurements include studies of temperature and composition dependence of conductivity, diffusion, viscosity, and density of electrolytes as well as electrochemical studies of electrolytes by cyclic voltammetry, electrochemical impedance spectroscopy, and cycling.

Prof. Dr. Gores is an active member of the Electrochemical Society, the International Society of Electrochemistry, the Bunsengesellschaft for Physical Chemistry, the Gesellschaft Deutscher Chemiker, the DECHEMA, the Society of Mining, Metallurgy and Exploration, and the Societé Française de Minéralogie et de Cristallographie.